A COMPARISON BETWEEN TWO DIFFERENT CFD APPROACHES OF A REAL SCROLL EXPANDER FOR MICRO-ORC APPLICATIONS

Alessio Suman[1,a], Carlo Buratto[1,2,b],
Nicola Aldi[1,c], Michele Pinelli[1,d], Pier Ruggero Spina[1,e]
Mirko Morini[3,*]

[1]Engineering Department in Ferrara (EnDiF), University of Ferrara, Ferrara, Italy
[2]Fluid-A s.r.l., Pieve di Cento, Bologna, Italy
[2]Industrial Engineering Department, University of Parma, Parma, Italy

[a] alessio.suman@unife.it, [b] carlo.buratto@unife.it, [c] nicola.aldi@unife.it, ,
[d] michele.pinelli@unife.it, [e] pier.ruggero.spina@unife.it

[*] mirko.morini@unipr.it

ABSTRACT

In this paper, CFD analyses of real scroll compressor are developed for a two-dimensional real geometry of a scroll compressor obtained by means of a Reverse Engineering (RE) of a commercial scroll compressor to be used as an expander in a microORC system. The analyses are carried out by means of CFD numerical simulations involving two type of approaches: (i) Dynamic Mesh (DM) and (ii) Chimera Strategy (CS). The particularity of these types of transient analyses consists in being able to reproduce the real operation of the machine through a sequence of relative positions between fixed and moving spirals. The results discuss the difference between the two numerical approaches in terms of ability to represent the actual flow features in a positive displacement machine. Analysis of the performance in terms of pressure and mass flow rate profiles, volumetric efficiency and shaft torque are reported.

1. INTRODUCTION

Scroll expander has recently become a good solution for micro and small scale ORC applications because of its reliability, compact structure, fewer moving parts, lower level of noise and vibration. Many experimental applications (up to 10 kW) can be found in literature (Bao and Zhao, 2013). In order to meet the increasing demands of efficiency and cost, the need for an experiment dedicated to each individual component of the energy system arose where the individual components are derived from applications other than those for which they are originally used. Laboratory micro- and sub-systems have been developed in order to study and optimize the entire energy system starting from *ad hoc* designed prototypes. In particular, a number of applications concerns small- and micro- size systems, for which the achievement of engineered solutions is particularly difficult. Bao and Zhao (2013) pointed out that for micro-energy system, the volumetric expander technology is the most preferable in terms of efficiency and cost. In particular, for applications in the range of (1 — 10) kWe, scroll, screw and rotary vane expanders are the most suitable for the ORC power-plants. The "*off-the-shelves"* availability of these components is very scarce and insufficient to meet the increasing demand of micro-scale component. In many cases, the designers have to be reinvented the volumetric expander taken from other applications (such as air condition, refrigeration, etc.). In these cases, the mathematical definition of the volumetric machine, that allows the preliminary analysis by studying the relationship between pockets evolution and the volumetric machine overall performance, is not possible. In this case, a new methodology, called Reverse Engineering (RE), represents a very useful method for generating a computational geometry of the real machine. The RE procedure and instruments have improved their accuracy in recent years and, at the same time, the progress in software development allows three-dimensional representation of the real object to be obtained in a very short time. The RE method has recently gained importance in product development, maintenance/recovery and remanufacturing fields (Bagci, 2009 and Gameros *et al.*, 2015). The application of RE approach is an ever increasing methodology in fluid machinery studies, but its application in conjunction with the CFD approach is the early stage when dealing with small size positive displacement machines.

In this paper, the real geometry of the commercial SANDEN TRSA09-3658 scroll compressor has been acquired. The scroll performance in the expansion mode was studied by means of a CFD numerical analysis. CFD applications to positive displacement machine have been increasingly proposed in literature (Song *et al.*, 2015), thanks to the evolution of capability both in terms of algorithms and computational resources and, in some cases, the CFD results could be used for setting up lumped parameter model (Ziviani *et al.*, 2014).

A very recent interesting review is presented in Song *et al.* (2015). In their work, the Authors states that CFD simulation for the scroll machine is still in early stage because of the complex geometry and unique motion of orbiting scroll wrap, which is also one of the main issues faced in the present paper. The CFD simulations, refer to a transient numerical simulation in which the computational mesh is modified (regenerated and/or moved) at each time step to accommodate the shape and size change of the gas pockets. The numerical simulations regard a two-dimensional or three-dimensional computational domain. The validity of 2D versus 3D simulation is still an open question. In fact, in Song *et al.* (2015) claim that 2D numerical models cannot reflect the accurate spatial distribution and variation of the flow field. At the same time, Chang *et al.* (2014), demonstrated that the pressure variation on the expansion process by 2D geometry is slightly higher than that of 3D model, but the overall tendency is similar and the deviation is acceptable.

The analyses presented in this paper consist of: (i) the acquisition of the scroll compressor Sanden TRSA09-3658 geometry through a RE procedure and its CAD reconstruction as an expander, (ii) the generation of the numerical domain in order to allows the CFD analysis by means of a two type of approaches, (iii) the transient simulation with the DM approach by using ANSYS Fluent, (iv) the transient simulation with the CS approach by using CD-ADAPCO STAR-CCM+ and (v) the analysis of the performance in terms of pressure and mass flow rate profiles volumetric efficiency and shaft torque. Both of the numerical strategies are able to reproduce the real operation of the machine through a succession of a relative positions between the fixed and moving profiles and the following variation of the scroll gas pocket size.

The CFD model allows the evaluation of the influence of leakage flows, e.g. due to radial (flank) gaps, which play a key role in the determination of the performances of the machine. Moreover, it allows the tuning of analytical and thermodynamic models with fewer resources in the design phase. For this reason, the computational effort and time represent a key parameter on this type of approach. This paper deals with this issues and compare two different numerical strategies for which the Authors will highlight differences and similarities of different CFD methods.

2. REAL SCROLL RECONSTRUCTION AND GEOMETRIC ANALYSIS

The real geometry of the Sanden TRSA09-3658 scroll was obtained through an RE procedure. The RE of the real component has been performed by means of a Romer laser scanner and the subsequent parametric CAD representations. At first, a 3D polygonal geometry of the real geometry is obtained by interpolating the point cloud derived from the laser scanner by means of the Polyworks V12 software.

In Tab. 1 the scroll geometrical characteristics are reported while in Fig. 1, a real scroll device is shown. As can be seen from Tab. 2, the scroll flank gaps are non-uniform flank gaps during the orbit. Some considerations can be drawn after the RE procedure:

- before RE, no evidence of variable-with-orbit flank gap was expected. Their variability observed on the actual machine, after RE, can be due to: (i) the functional discrepancy between ideal CAD geometry and actual geometry after manufacturing; (ii) the actual geometry of the stator and

Table 1: Scroll compressor characteristics

Volume ratio	3.1055	
Maximum inlet volume [mm^3]	85,900	
Spiral height [mm]	33.5	
End-plate diameter [mm]	120.0	
Axial duct diameter [mm]	12.0	
Radial duct diameter [mm]	12.5	
Flank gap [µm]	**0° (inlet chambers close)**	20
	90°	36
	180°	94
	270°	36

rotor assembly during standard working operation; (iii) the error inherent to the laser scanner device and to the subsequent interpolating process of the cloud points;

- the maximum inlet volume of the Sanden scroll compressor delivered by the manufacturer is different from the measured one. In particular, the manufacturer value is equal to 85,700 mm^3. The discrepancy between the two values are equal to 200 mm^3. After an order of magnitude calculation, this value was estimated to be equivalent to an uncertainty on the mass flow rate of about 1.5 %, which is acceptable if compared to typical experimental uncertainty on mass flow rate as reported by Matos and Rodrigues (2013).

The reproduction of the scroll as obtained by RE is shown in Fig 1 where the scroll profile is made regular and continuous by means of Spline curves. The CAD geometry of the real scroll is then exported in the CAD software SolidWorks through an interchange file format, e.g .stp or .iges format.

The computational domain consists of a bi-dimensional representation of the scroll machine. A 2D section has been obtained by intersecting the 3D polygonal model with a plane perpendicular to the rotation axis. In Fig. 2a, the 2D surface used for CFD simulation is outlined. To perform the subsequent 2D CFD simulation, the outlet boundary condition has been imposed in correspondence to the outlet duct (right-top duct in Fig. 2a), while the inlet boundary condition has been imposed in correspondence to the central volume of the machine by means of an opening on the fixed profile. In Fig. 2b, the detail of the central volume of the scroll in which the inlet section has been placed is presented. This numerical domain will use for both numerical analysis (DM and CS).

The 2D numerical domain uses the actual flank gaps derived from the RE. The consequent numerical simulation has to allow the resolution of the numerical model when very small (always lower than 100 µm with a minimum as equal to 20 µm) and variable-with-orbit flank gaps afflicted the scroll operation. For this reason the computational mesh e the transient simulation have to be accurately defined.

Figure 1: Scroll Sanden TRSA09-3658

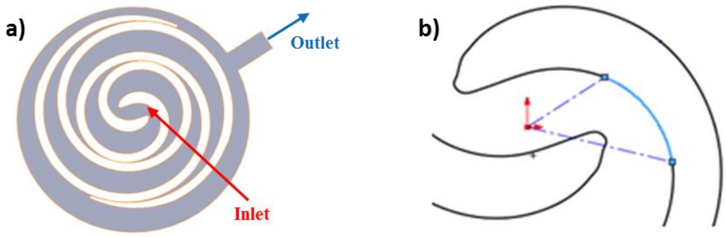

Figure 2: 2D Numerical domain

3. DYNAMIC MESH APPROACH

Since the scroll machine operation is based on the variation of the gas pocket volume according to the crack shaft position, the numerical domain and the resolution strategy are developed in order to accommodate this process. Two different numerical approaches are adopted and compared.

3.1 Dynamic mesh approach

The CFD simulations were carried out as a 2D transient numerical model by using a Dynamic Mesh (DM) strategy implemented in ANSYS Fluent 13.0. This transient analysis is able to reproduce the real operation of the machine through a sequence of relative positions between the fixed and moving profile by imposing an angular increment.

The use of 2D CFD analysis by using a DM for studying some particular fluid dynamic phenomena in the gear pumps. In particular, Castilla *et al.* (2010) put the attention to the turbulence structure in the suction chamber, while Del Campo *et al.* (2012) analyzed the pressure variation and cavitation phenomena. In these cases, the 2D strategy allows the comprehension of the major fluid dynamic phenomena involved in volumetric devices.

In this paper, with the DM strategy, the mesh inside the fixed and moving (orbiting) profiles is regenerated at each time step to accommodate the shape and size change of the gas pockets. The mesh regeneration could follow element size criteria and/or element quality criteria (such as skweness).

The numerical domain of the real scroll is discretized through the use of a triangular mesh. The mesh was composed of about 900,000 triangular elements. The maximum element skewness of the initial mesh is smaller than 0.33 (0.60 before smoothing) and a minimum orthogonal quality at least equal to 0.655 was achieved. To increase the resolution of the mesh close to the walls, a local mesh refining approach was adopted. The local refining around the walls is shown in Fig. 3. In the flank gap there are at least two triangular mesh elements in agreement with the data reported in literature (Castilla *et al.*, 2010 and Del Campo *et al.*, 2012) for volumetric displacement.

3.1 Chimera approach

Overlapping grid, subsequently named the Chimera approach, was first introduced in the early

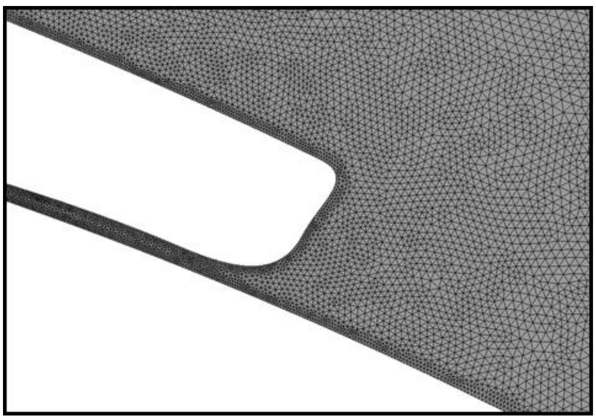

Figure 3: Local mesh refinement around the scroll edge in the case of DM strategy

1980's (Steger and Benek, 1987) when several grid assembly packages have become available (Roget and Sitaraman, 2014). In the present paper, the simulation of the scroll expander with the Chimera Strategy (CS) was carried out by means of CD-ADAPCO STAR-CCM+ 9.04. The overset method consist in the contemporary use of active cells and passive cells. In active cells, regular discretized equations are solved, while in passive cells, no equation is solved, they are temporarily or permanently de-activated. Active cells along interface to passive cells refer to donor cells at another grid instead of the passive neighbors on the same grid. The first layer of passive cells next to active cells are called acceptor cells. The solution is computed on all grids simultaneously. Grids are implicitly coupled through the linear equation system matrix. Different interpolation functions can be used to express values at acceptor cells via values at donor cells. The donor cells must be active cells, and the change of cell status is automatically controlled by the solver. Overset grids usually involve one background mesh, which is adapted to environment, and one or more overset grids attached to bodies, overlapping the background mesh and/or each other as reported in Fig. 4. Each grid (background and overset) can move according to the motion models implemented in the CFD software. In literature, the comparison between the CS and other CFD strategies are limited. Togasci *et al.*, 2001 and Hoke *et al.*, 2009 report the applications of the overset grid for a rocket booster and a 2D airfoil, respectively. Comparison with experimental data (Togasci *et al.*, 2001) and other CFD solutions (Hoke *et al.*, 2009) demonstrated that the CS is reliable for different fluid dynamics applications. The major difference with respect to the DM approach consists that CS does not deform the mesh during the calculation.

In the present paper the background mesh and the overlapping mesh are reported in Fig. 5. The overlapping mesh bounded the moving scroll spiral and are obtained by an offset of 1.5 mm from the actual moving scroll spiral. Overlapping mesh is made up with 171,073 elements while the background mesh (that refers to the scroll stator and fixed spiral) is made up by 529,547 elements. Overlapping and background mesh are constitute by polyhedral elements and prism layer close to the wall. In the particular reported in Fig. 5 clearly visible are the polyhedral elements in the core regions while the prism layer close to the wall allow the grid refinement and the good representation of the flank leakage.

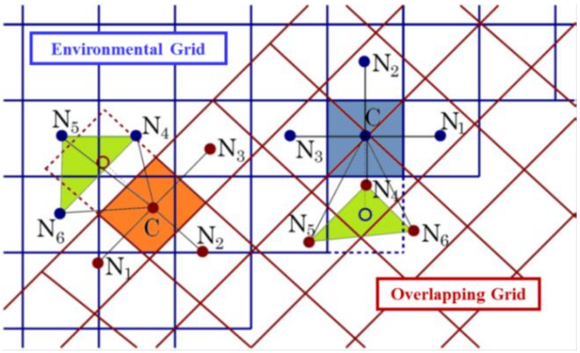

Figure 4: N_1, N_2, N_3 neighbors from same grid; N_4, N_5, N_6 neighbors from overlapping grid (Schreck and Perić, 2012)

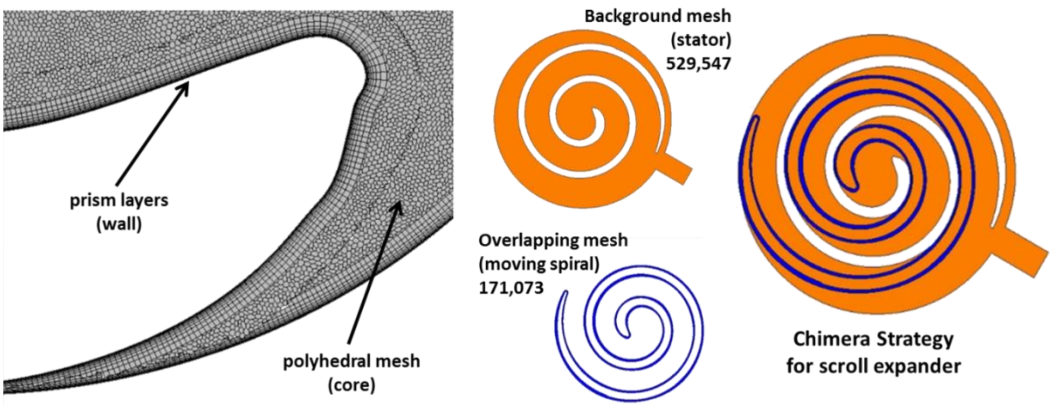

Figure 5: Background and overlapping mesh

5. COMPARISON

5.1 Boundary conditions

To perform a comparative analysis, the same boundary conditions were applied in the two numerical simulations. To perform the two-dimensional CFD simulations, the inlet boundary condition has been imposed in correspondence to the central volume of the machine by means of an opening on the fixed profile as reported in Fig. 2b. Both simulations (DM and CS) were conducted by imposing a pressure ratio of 3.5. The reference pressure is 101,325 Pa. The rotational velocity was imposed equal to 2,000 rpm. The turbulence model chosen, in accordance with Cui (2006), is the k-ε model combined with standard wall functions. The fluid considered for the comparisons between the DM and CS simulation is air at standard conditions. Simulation of scroll machines by using real gas equations is numerically very challenging and could drain most of the computational resources during the simulation. Moreover, the specific geometry under consideration is characterized by time-varying sliding narrow gaps which result in tough convergence issues when using air as the working fluid. These issues are even more relevant when refrigerant is used. For these reasons, for the purposes of this paper (i.e. sensitivity analyses and the comparison between two different simulation strategies) only air is considered as the working fluid. The time step of the transient analyses is equal to $5.21 \cdot 10^{-6}$ s that corresponds to an angular increment of 0.0625° of the scroll crank. The advection scheme adopted for both analyses is the second order Upwind.

5.2 Pressure field and fluctuations at the ports

In Fig. 6, the trends of the inlet chamber pressure of the scroll expander are presented as a function of the normalized angular position of the orbit covered by the moving spiral profile. The solution provided by the CS shows a smooth trend in discharge pressure even if, the pressure fluctuation showed by the DM solution (at 3/4 of the orbit) is contained in few Pa (less than 0.75 %).

Comparing the contour plots referring to the latter expander orbits angles (3/4 and 1) DM and CS solutions show a different pressure for the twin discharge pockets. This phenomenon is related to the asymmetric position of the inlet and outlet ports and strongly linked to the design of the scroll machine even if in the Chimera Strategy this phenomenon is less appreciated. Pressure fields are comparable and clearly visible, in both solutions, are the pressure evolutions inside the isolated pockets: (i) the inlet pocket (which the pressure graph referred), (ii) the intermediate pocket and finally (iii) the discharge pocket and the outlet duct.

The pressure trends and the pressure field representation allow the definition of which pressure fluctuations affect the machine during standard operation. These results are very important to understand the vibration and noise generated by the machine.

5.3 Flow rate and velocity field

In Fig. 7, the trends of the mass flow of the scroll expander are reported as a function of the normalized angular position of the orbit covered by the moving spiral profile. The trends of the mass flow rate are very similar in both of the scroll expander ports. In the inlet section, the same mass flow rate fluctuation can be observed for the two numerical strategies. The higher mass flow rate operated

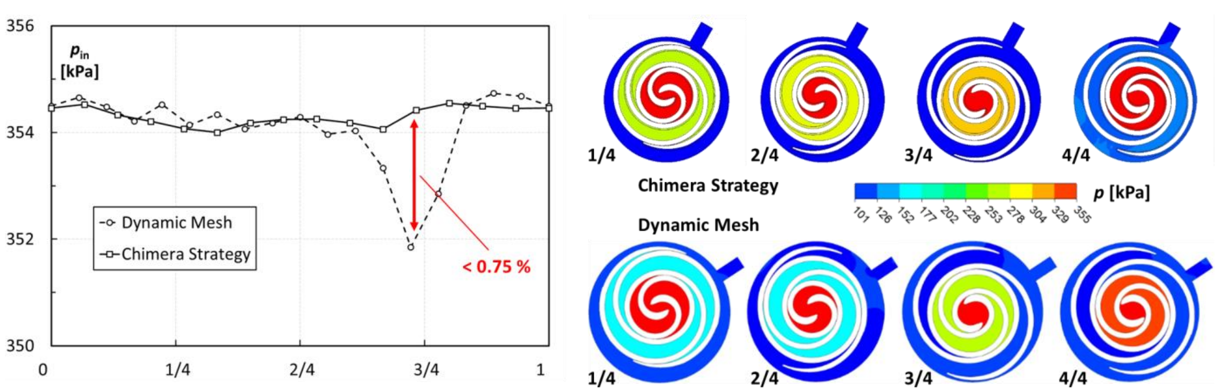

Figure 6: Inlet pressure and pressure fields during the orbits

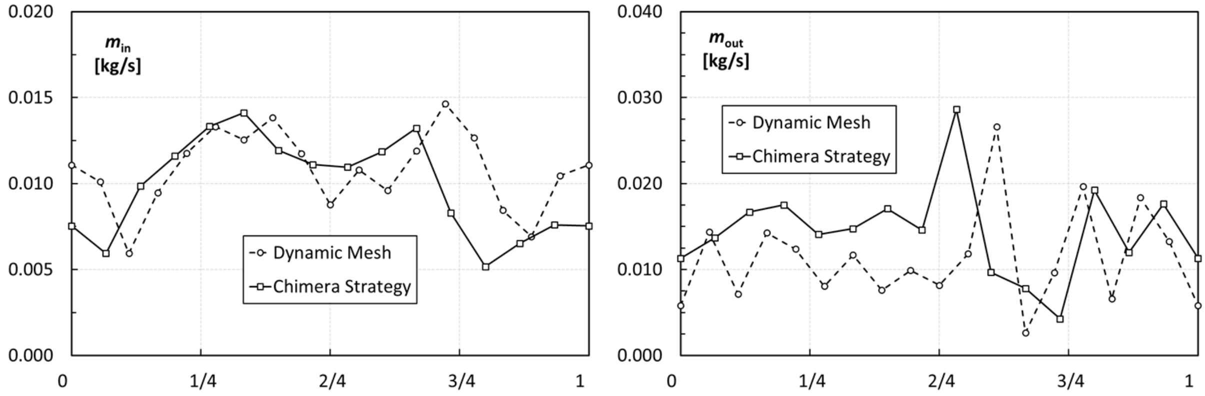

Figure 7: Mass flow rate

by the scroll expander in the orbit angle range from 1/4 to 3/4 is due to the position of the moving spiral that is in the opposite position with respect to the inlet port. This phenomenon is well described by the two numerical strategies. The average values of the inlet mass flow rate are: (i) 0.0108 kg/s in the DM solution and (ii) 0.0098 kg/s in the CS solution. The deviation is equal to 0.001 kg/m s that corresponds to the 9 % with respect to the higher value. Considering the (i) different numerical approaches that reflect in different mesh topology, (ii) different solution strategies and (iii) the scroll machine peculiarities, these values are considered acceptable.

Regarding the discharge mass flow rate, same consideration can be done. The fluctuations is well reproduced by the two strategies even if the CS solution shows a higher values in the first half of the scroll orbit. Pressure fluctuations reported above and mass flow rate discontinuities are due to interaction between the moving spiral and the outlet port positioned closer to the upper gas pocket (as can be seen in Fig. 2). Comparing the phase of the two mass flow rate trends it is possible to note the phase shift. Chimera Strategy solution appears in advance with respect to the DM solution for the inlet mass flow rate trend and for the outlet mass flow rate trend up to 2/4 orbit. However, in the last part of the orbit, in the case of outlet mass flow rate the DM solution appears in advance with respect to the CS solution. The difference highlighted for the mass flow rate values are due to resolution of the flank gaps that allow the fluid in the scroll expander to by-pass the moving scroll towards the discharge outlet. The mesh refinement close to the walls (realized in both cases) are able to describe this phenomenon as can be seen in Fig. 8, but, due to the different numerical approach, the global solution of this local fluid dynamic phenomenon is different. In Fig. 8 there are two representations of the flank leakage that affect the scroll expander. In this operation mode, the fluid overpasses the spiral through the flank gaps without energy exchanges (and thus work) with the mobile spiral. Figure 8 shows the flank leakages (i) from the discharge chamber to the outlet volume (casing), (ii) from the expansion chamber to the discharge chamber and finally (iii) from the suction chamber to the expansion chamber. In Fig. 9, the evolution of the velocity fields inside the expander scroll are presented. From these plots, the back flow at the inlet port during compression mode can be clearly observed. This aspect seems to be due to the dimension of the external case of the scroll machine. This result may not be very representative of the actual scroll machine. In fact, in these bi-dimensional simulations the operation fluid does not have the possibility to move along the rotating axis of the machine, and thus, possible three dimensional flows are neglected from the results reported in this paper.

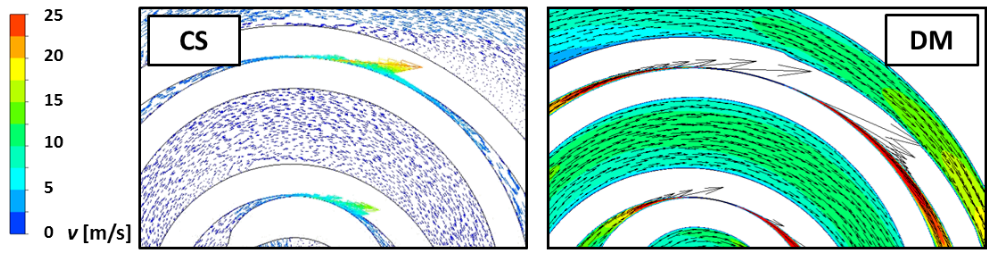

Figure 8: Flank leakage in the scroll expander

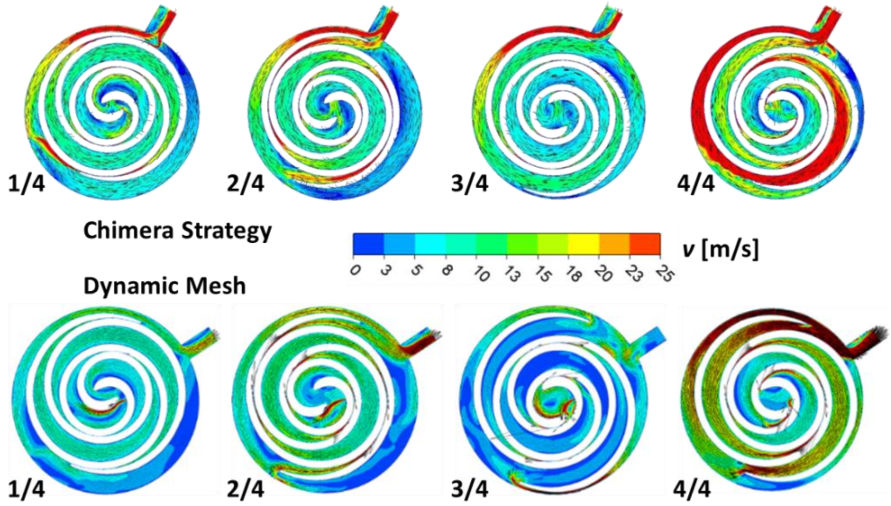

Figure 9: Velocity fields

5.4 Shaft torque and volumetric efficiency

The comparison between the two numerical approaches was carried out also by the scroll performance. Starting from the CFD results, in this paragraph the authors have reported the scroll performance related to (i) shaft torque and (ii) volumetric efficiency.

Figure 10 reports the shaft torque trends for CS and DM simulations. Also in this case, the two shaft torque trend as a function of the normalized angular position of the orbit covered by the moving spiral profile are very consistent to each other. The shaft torque generated by the moving spiral varying in the range form 2.20 Nm to 0.35 Nm. The CS solution shows a more smooth trend. The pressure and mass flow rate fluctuations highlighted in correspondence of the position equal to 3/4 of the orbit angle determine a shaft torque variation, especially in the DM solution.

The volumetric efficiency of the scroll machine was also estimated by means of CFD results for both of the solutions. The volumetric efficiency of the scroll expander, VFM (Volumetric Flow Matching ratio), was obtained as the ratio of the ideal volume flow rate determined through the theoretical volume isolated by the scroll and the CFD calculated volume flow operated by the scroll. The VFM value should be as close as possible to one for optimal performance. Greater values indicate higher volumetric losses.

The VFM resulted equal to (i) 3.06 in the case of DM solution and (ii) 2.80 in the case of CS solution. The deviation is due to the deviation highlighted for the values of the mass flow rate at the expander inlet port. These high values, consistent with the data presented by Mathias *et al.* (2009), are closely related to the value of the flank gap imposed between the fixed scroll and the moving scroll. As previously mentioned, the magnitude of the flank gap influences the performance of the scroll machine (in particular the volumetric efficiency). By using the CFD simulations, leakage flows in the flank gap, that affect the operation of both machines, can be clearly observed as reported in Fig. 8.

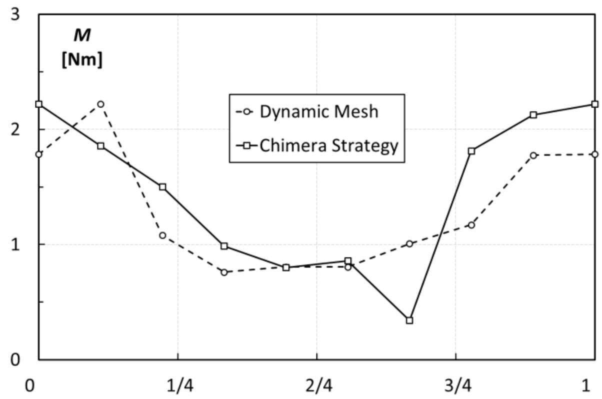

Figure 10: Shaft torque

The flank leakages are, in general, driven by (i) the magnitude of the flank gaps, (ii) the density of the operating fluid, (iii) the presence of the lubricating oil and (iv) the pressure difference between two consecutive isolated pockets. In general long spirals allow the reduction of the pressure difference between two consecutive isolated pockets (and thus there is less flank leakage) but the scroll machine becomes bigger and more expensive. In the same way, the use of lubricating oil allows the reduction of leakages thanks to its phase (liquid) and viscosity but the scroll machine and, in this case, the entire circuit become more complicated and expensive.

6. CONCLUSIONS

In this paper a comprehensive performance and fluid dynamic assessment of a real scroll machine was presented by means of CFD analyses. The numerical analysis based on the comparison between two different numerical approaches for the analysis of a real scroll machine used as an expander.

Thanks to the use of a reverse engineering procedure, an unknown scroll compressor geometry was reconstructed and digitalized. The use of CFD simulation allows the study of the detailed working features of the machine that are not completely visible with other types of analyses (such as thermodynamic or lumped approach). Two CFD methods were developed by means of a transient numerical simulations. Dynamic mesh approach and Chimera Strategy are used in order to reproduce the real operation of the machine through a sequence of relative positions between fixed and moving spirals. The CFD transient simulations allowed the evaluation of time profile of the mass flow rate and pressure fluctuations at the inlet and outlet sections of the machine.

The comparison between the two numerical strategies on a real scroll machine was carried out through the analysis of (i) pressure field inside the scroll pocket, (ii) the mass flow rate at the inlet and outlet ports, (iii) velocity field and the influence of the flank gap and finally (iv) shaft torque and volumetric efficiency.

Results show that both of numerical strategies are able to reproduce the pressure fluctuation (deviation less than 0.75 % at the inlet port) and the mass flow rate variation at the ports. Differences were highlighted for the phase of fluctuations of the mass flow rate trend. Scroll expander performance such as shaft torque and volumetric efficiency are very consistent between the two numerical strategies.

The capability of the two approaches to calculate the pressure and mass flow rate fluctuations represent a key results and both of this method could represent an very useful tool during the design phase. All of fluid dynamic phenomena impact on the scroll performance, and only through their comprehension it is possible to optimize the scroll design by the modification of the spiral profile or the position and dimension of the inlet and outlet port. Pressure fluctuations are closely related to vibrations and noise generated by the machine in operation.

NOMENCLATURE

M	torque	[Nm
m	mass flow rate	[kg/s]
N	grid node	
p	pressure	[Pa]
v	velocity	[m/s]

Subscript

in	inlet
out	outlet

Acronyms

CFD	Computational Fluid Dynamics
CS	Chimera Strategy
DM	Dynamic Mesh

RE Reverse Engineering
VFM Volumetric Flow Matching ratio

REFERENCES

Bagci, E., 2009, Reverse engineering applications for recovery of broken or worn parts and re-manufacturing: Three case studies, *Adv. Eng. Software*, **40**, pp. 407-418.
Bao, J., Zhao, L., 2013, A review of working fluid and expander selections for organic Rankine cycle", *Renewable and Sustainable Energy Rev.*, **24**, pp. 325-342.
Castilla, R., Gamez-Montero, P. J., Ertürk, N., Vernet, A., Coussirat, M., Codina, E., 2010, Numerical simulation of turbulent flow in the suction chamber of a gear pump using deforming mesh and mesh replacement, *Int. J. Mech. Sci.*, **52**, pp. 1334-1342.
Chang, J. C., Chang, C. W., Hung, T. C., Lin, J. R., Huang, K. C., 2014, Experimental study and CFD approach for scroll type expander used in low-temperature organic Rankine cycle, *Appl. Therm. Eng.*, **73**, pp. 1444-1452.
Cui, M. M., 2006, Numerical Study of Unsteady Flows in a Scroll Compressor, *J. Fluids Eng.*, **128**, pp. 947-55.
Del Campo, D., Castilla, R., Raush, G. A., Gamez-Montero, P. J., Codina, E., 2012, Numerical Analysis of External Gear Pumps Including Cavitation, *J. Fluids Eng.*, **134**, p. 081105.
Gameros, A., De Chiffre, L., Siller, H. R., Hiller, J., Genta, G., 2015, A reverse engineering methodology for nickel alloy turbine blades with internal features, CIRP *J. Manuf. Sci. Technol*., art. in press (9 pages).
Hoke, C., Decker, R., Cummings, R., McDaniel, D., Morton, S., 2009, Comparison of Overset Grid Deformation Techniques Applied to 2-Dimensional NACA Airfoils, 19th AIAA Computational Fluid Dynamics Conference, 22 - 25 June 2009, San Antonio, Texas, US.
Mathias, J. A., Johnston, J. R. J., Cao, J., Priedeman, D. K., Christensen, R. N., 2009, Experimental Testing of Gerotor and Scroll Expanders Used in, and Energetic and Exergetic Modeling of, an Organic Rankine Cycle, *J. Energy Res. Technol.*, **131**, p. 012201.
Matos, M. A., Rodrigues, N., 2013, Gas mass-flow meters: Measurement and uncertainties, *Flow Meas. Instrum.*, **33**, pp. 45-54.
Roget, B., Sitaraman, J., 2014, Robust and efficient overset grid assembly for partitioned unstructured meshes, J. Comput. Phys., **260**, pp. 1-24.
Schreck, E., Perić, M., 2012, Overset Grids in STAR-CCM+: Methodology, Applications and Future Developments, STAR Japanese Conference 2012.
Song, P., Wei, M., Shi, L., Danish, S. N., Ma, C., 2015, A review of scroll expanders for organic Rankine cycle systems, *Appl. Therm. Eng.*, **75**, pp. 54-64.
Steger, J. L., Benek, J. A., 1987, On the use of composite grid schemes in computational aerodynamics, *Comput. Methods Appl. Mech. Eng.*, **64**, pp. 301–320.
Togashi, F., Nakahashi, K., Ito, Y., Iwamiya, T., Shimbo Y., 2001, Flow Simulation of NAL Experimental Supersonic Airplane/Booster Separation Using Overset Unstructured Grids, *Comput. Fluids*, **30**(6), pp. 673-688.
Ziviani, D., Suman, A., Lecompt, S., De Paepe, M., van den Broek, M., Spina, P. R., Pinelli, M., Venturini, M., Beyene, A., 2014, Comparison of a Single-Screw and a Scroll Expander under Part-Load Conditions for Low-Grade Heat Recovery ORC Systems, Proc. of 6th International Conference on Applied Energy (ICAE2014), Taipei, 30 May - 2 June, 2014, Paper n. 78, pp. 1-4.

ACKNOWLEDGEMENT

The research was partially supported by the Italian Ministry of Economic Development within the framework of the Program Agreement MSE-CNR "Ricerca del Sistema elettrico nazionale (RdS)".